Biol. Cybern. 89, 289–302 (2003)
DOI 10.1007/s00422-003-0400-3

Biological Cybernetics

Partial correlation analysis for the identification of synaptic connections

Michael Eichler[1], **Rainer Dahlhaus**[1], **Jürgen Sandkühler**[2]

[1] Institut für Angewandte Mathematik, Universität Heidelberg, Im Neuenheimer Feld 294, 69120 Heidelberg, Germany
[2] Brain Research Institute, Vienna University Medical School, Spitalgasse 4, 1090 Vienna, Austria

Received: 2 August 2002 / Accepted: 28 January 2003 / Published online: 14 October 2003

Abstract. In this paper, we investigate the use of partial correlation analysis for the identification of functional neural connectivity from simultaneously recorded neural spike trains. Partial correlation analysis allows one to distinguish between direct and indirect connectivities by removing the portion of the relationship between two neural spike trains that can be attributed to linear relationships with recorded spike trains from other neurons. As an alternative to the common frequency domain approach based on the partial spectral coherence we propose a new statistic in the time domain. The new scaled partial covariance density provides additional information on the direction and the type, excitatory or inhibitory, of the connectivities. In simulation studies, we investigated the power and limitations of the new statistic. The simulations show that the detectability of various connectivity patterns depends on various parameters such as connectivity strength and background activity. In particular, the detectability decreases with the number of neurons included in the analysis and increases with the recording time. Further, we show that the method can also be used to detect multiple direct connectivities between two neurons. Finally, the methods of this paper are illustrated by an application to neurophysiological data from spinal dorsal horn neurons.

1 Introduction

Major progress has been made in understanding the functions of the nervous system on molecular, cellular, and systemic levels. In contrast, the organization and function of local neuronal networks are largely unknown. With the exception of the retina, the goal of relating network connectivity to function has not been achieved in any area of the vertebrate nervous system. Thus, a major challenge of future neuroscience will be to approach the complex interplay of functionally connected ensembles of neurons.

Functionally relevant neuronal connections can be defined and identified by changes in discharge probability in a postsynaptic neuron by activity in excitatory or inhibitory presynaptic neurons. While direct, i.e., monosynaptic, connections are devoid of interneurons, polysynaptic pathways involve one or more intercalated neurons. A number of experimental methods are now available to simultaneously record action potential discharges of large numbers of neurons. These include multiple single-neuron recordings with an array of microelectrodes (Krüger 1983) or tetrodes (Gray et al. 1995), confocal calcium imaging (Fetcho and O'Malley 1995), multisite recordings from cultured neurons with planar electrode arrays (Maeda et al. 1995), or multiple single-neuron recordings with voltage sensitive dyes (Grinvald et al. 1988).

Any reliable description of neuronal network function needs to identify excitatory vs. inhibitory and monosynaptic vs. polysynaptic connections. The neurophysiological identification of synaptic connections is typically based on the recorded times of discharges of the neurons under study. The association between such neural spike trains is commonly measured by the cross-correlation histogram (Perkel et al. 1967), which is the histogram of the times of occurrence of all output spikes relative to the times of occurrence of all input spikes. The peaks and troughs in such histograms indicate the change of probability for the occurrence of an output spike due to the presence of an input spike, thus revealing the type and the time delay of the synaptic connection. However, when analyzing the structure of a larger neural ensemble we cannot infer from the cross-correlation histogram to what extent these changes are due to a direct connection between the two neurons, to indirect connections via other recorded neurons, or to common inputs.

A frequency domain approach based on the method of linear partialization has been discussed by Brillinger

Correspondence to: M. Eichler
(e-mail: eichler@statlab.uni-heidelberg.de,
Tel.: +49-6221-548970, Fax: +49-6221-545331)

et al. (1976), Rosenberg et al. (1989), and Dahlhaus (2000) for neurophysiological data. Although the method allows one to distinguish direct from indirect connections, no distinction is made between excitatory and inhibitory connections.

In this paper, we present a partialization analysis in the time domain. The method is based on a scaled version of the partial covariance density, which can be estimated by frequency domain methods. The scaled partial covariance density combines the advantages of the crosscorrelation histograms and the partialization analysis in the frequency domain. In particular, it can be interpreted in the same way as the crosscorrelation histograms with peaks and troughs indicating excitatory and inhibitory connections, while on the other hand it allows for the discrimination of direct and indirect connections and common inputs. The theoretical background is presented in Sect. 2. In Sect. 3, the results from a simulation study are given. Furthermore, the method is applied to a data set consisting of ten spike trains from spinal dorsal horn neurons.

2 Methods

2.1 Multivariate point processes

The method discussed in this section is entirely based on the relation between the sequences of times of occurrence of discharges recorded from different neurons. Therefore, these neural spike trains can be represented by stochastic point processes. A point process in general refers to an ordered sequence of isolated events $\{\tau_j\}_{j\in\mathbb{Z}}$ occurring randomly in time. Such a point process associated with the spike train of neuron a can be represented by the counting process $N_a(t)$, where $N_a(t)$ is the total number of action potentials of neuron a from time 0 up to time t. For the details about point processes we refer to the monographs of Cox and Isham (1990) and Daley and Vere-Jones (1988).

Subsequently, it will be assumed that the multivariate point process N is stationary, that is, its properties are independent of the time at which the process is observed. We further assume that increments of the process N well separated in time are independent and, finally, that the points of the process do not occur simultaneously.

The connectivities between neurons are commonly studied by pairwise second-order statistics. In the time domain, the conditional intensity function $m_{ab}(u)$ describes the probability of occurrence of a spike of type a at time $u > 0$ given that a spike of type b has occurred at time 0

$$m_{ab}(u) = \text{Prob}\{\mathrm{d}N_a(u) = 1 | N_b(0) = 1\}/\mathrm{d}u$$

where $\mathrm{d}N_a(t) = N_a(t+\mathrm{d}t) - N_a(t)$. Alternatively, one might consider the cross-covariance density at lag u between processes N_a and N_b:

$$q_{ab}(u) = \text{cov}\{\mathrm{d}N_a(t), \mathrm{d}N_b(t+u)\}/(\mathrm{d}t\,\mathrm{d}u) \tag{1}$$

which is related to the conditional intensity function by $q_{ab}(u) = m_{ab}(u)p_b - p_a p_b$, where $p_a = \text{Prob}\{\mathrm{d}N_a(t) = 1\}/\mathrm{d}t$ is the mean intensity of process N_a. Since the increments $\mathrm{d}N_a(t)$ of a point process are discrete with values of only 0 or 1, it follows that $\text{var}\{\mathrm{d}N_a(t)\} = p_a\mathrm{d}t$ and, consequently, the right-hand side of Eq. 1 does not converge for $\mathrm{d}t, \mathrm{d}u \to 0$ if $a = b$ and $u = 0$. In this situation, the autocovariance density q_{aa} is defined such that it is continuous also at $u = 0$. Because of this behavior of the variance the correlation

$$\text{corr}\{\mathrm{d}N_a(t), \mathrm{d}N_b(t+u)\} = \sqrt{\mathrm{d}t\,\mathrm{d}u}\,\frac{q_{ab}(u)}{\sqrt{p_a p_b}}$$

for $u \neq 0$ or $a \neq b$ converges to 0 as $\mathrm{d}t, \mathrm{d}u \to 0$. The expression, however, suggests that the following scaled covariance density (SCD)

$$s_{ab}(u) = \frac{q_{ab}(u)}{\sqrt{p_a p_b}}$$

be used as a measure for the linear dependence of the two processes N_a and N_b. This statistic is not bounded like an ordinary correlation but still has a number of useful properties. For example, in the case of Hawkes' self-exciting processes (Hawkes 1971a,b), which have linear relationships, the scaled covariance densities stay constant if the mean intensities of all component processes are increased by a common factor. We note that van den Boogaard et al. (1986) used a different scaling for the covariance density that, however, has been motivated only by giving particularly simple expressions for the second-order dependencies in the discussed neuron model.

In the frequency domain, the corresponding second-order parameters are the cross spectrum between processes N_a and N_b:

$$f_{ab}(\lambda) = \frac{1}{2\pi}\int_{-\infty}^{\infty} q_{ab}(u)\exp(-\mathrm{i}\lambda u)\,\mathrm{d}u$$

and for $a = b$ the autospectrum $f_{aa}(\lambda)$

$$f_{aa}(\lambda) = \frac{p_a}{2\pi} + \frac{1}{2\pi}\int_{-\infty}^{\infty} q_{aa}(u)\exp(-\mathrm{i}\lambda u)\,\mathrm{d}u$$

The association between two processes N_a and N_b is measured by the spectral coherence $|R_{ab}(\lambda)|^2$ where

$$R_{ab}(\lambda) = \frac{f_{ab}(\lambda)}{\sqrt{f_{aa}(\lambda)f_{bb}(\lambda)}}$$

The spectral coherence is bounded and takes values between 0 and 1. Let $d_a^{(T)}$ denote the finite Fourier transform of process N_a:

$$d_a^{(T)}(\lambda) = \int_0^T h(t/T)\exp(-\mathrm{i}\lambda t)\,\mathrm{d}N_a(t)$$

where h is a data taper (cf. Brillinger 1981). Then the spectral coherence satisfies

$$|R_{ab}(\lambda)|^2 = \lim_{T\to\infty} \left|\mathrm{corr}\{d_a^{(T)}(\lambda), d_b^{(T)}(\lambda)\}\right|^2$$

If the spectral coherence vanishes for all frequencies, the two spike trains are linearly independent, whereas a value of one indicates a perfect linear relationship between the two processes.

If the process has been observed on the interval $[0, T]$, the estimates for the second-order parameters in the time domain are typically based on the crosscorrelation histogram:

$$\hat{m}_{ab}(u) = \frac{\#\{(j,k)|u-h<\sigma_j-\tau_k<u+h; \sigma_j\neq\tau_k\}}{2hN_b(T)}$$

where "#" stands for "the number of" and $\{\sigma_j\}$ and $\{\tau_k\}$ denote the observed spike times for neuron a and b, respectively, up to time T. In the frequency domain, the finite Fourier transform $d_a^{(T)}$ can be computed efficiently at the Fourier frequencies $\lambda_j = 2\pi j/T$ by a fast Fourier algorithm based on a discrete approximation of the process N_a (Rigas 1992). The spectral density matrix $f(\lambda) = \left(f_{ab}(\lambda)\right)_{a,b=1,\ldots,d}$ can then be estimated componentwise by

$$f_{ab}^{(T)}(\lambda) = \frac{1}{2\pi H_2 T}\sum_{j\in\mathbb{Z}} w^{(T)}(\lambda-\lambda_j) d_a^{(T)}(\lambda_j) d_b^{(T)}(-\lambda_j)$$

where $H_k = \int_0^1 h(t)^k \mathrm{d}t$, $w^{(T)}(\lambda) = M_T w(M_T\lambda)$ for some sequence $M_T \to \infty$, and w is some kernel function with bounded support (Brillinger 1981). A more detailed discussion of frequency methods may be found in Brillinger et al. (1976) and Rosenberg et al. (1989).

2.2 Partial correlation analysis

When analyzing the structure of a larger neural net, the question arises as to what extent the association between two processes N_a and N_b is due to a direct connection between the two neurons or whether the observed correlation can be attributed to an indirect connection involving other neurons, say, $c_1, \ldots, c_r$, or is only due to a common input from these neurons. This question can be addressed by second-order statistics using the method of partialization. The basic idea is to measure the association between the two processes N_a and N_b after the linear effects of the multivariate process $N_C = (N_{c_1}, \ldots, N_{c_r})'$ have been subtracted. It is clear that in this approach the meaning of direct and indirect connections depends on the measured network and that the inclusion of any additional neurons may lead to the identification of a formerly direct connection as being indirect.

Brillinger et al. (1976), Rosenberg at al. (1989), and Dahlhaus et al. (1997) have discussed the partialization analysis in the frequency domain and recommended the use of the partial spectral coherence $|R_{ab|C}(\lambda)|^2$ where

$$R_{ab|C}(\lambda) = \frac{f_{ab|C}(\lambda)}{\sqrt{f_{aa|C}(\lambda) f_{bb|C}(\lambda)}}$$

with the partial spectral densities

$$f_{ab|C}(\lambda) = f_{ab}(\lambda) - f_{aC}(\lambda) f_{CC}(\lambda)^{-1} f_{Cb}(\lambda) \tag{2}$$

Let $\hat{N}_{a|C}(t)$ be the best predictor of $N_a(t)$ based on the process N_C, which is given by

$$\hat{N}_{a|C}(t) = \mu + \int_0^t \int_{-\infty}^{\infty} \phi(s-u)\,\mathrm{d}N_C(u)\,\mathrm{d}s$$

where ϕ has Fourier transform $\hat{\phi}(\lambda) = f_{aC}(\lambda) f_{CC}(\lambda)^{-1}$ and $\mu = p_a - \hat{\phi}(0) p_C$. We can then define the partial residual process

$$\varepsilon_{a|C}(t) = N_a(t) - \hat{N}_{a|C}(t)$$

The association between N_a and N_b after removing the linear effects of N_C can now be described by the corresponding second-order parameters of the partial residual processes $\varepsilon_{a|C}$ and $\varepsilon_{b|C}$. For example, the partial spectral coherence can be seen to be the correlation between the Fourier transforms $d_{a|C}^{(T)}$ and $d_{b|C}^{(T)}$ of the partial residual processes $\varepsilon_{a|C}$ and $\varepsilon_{b|C}$:

$$|R_{ab|C}(\lambda)|^2 = \lim_{T\to\infty} \left|\mathrm{corr}\{d_{a|C}^{(T)}(\lambda), d_{b|C}^{(T)}(\lambda)\}\right|^2$$

In the time domain, we can similarly define the partial covariance density of N_a and N_b by

$$q_{ab|C}(u) = \mathrm{cov}\{d\varepsilon_{a|C}(t+u), d\varepsilon_{b|C}(t)\}$$

which is related to the partial cross-spectral density by

$$q_{ab|C}(u) = \int_{-\infty}^{\infty} f_{ab|C}(\lambda)\exp(-\mathrm{i}\lambda u)\,\mathrm{d}\lambda$$

Similarly, the partial autocovariance density $q_{aa|C}$ is the Fourier transform of $f_{aa|C}(\lambda) - p_a/2\pi$, where the second term corresponds to the variation of the increments of the partial residual process $\varepsilon_{a|C}$. Since the best predictor $\hat{N}_{a|C}$ is continuous in time, the variation of $d\varepsilon_{a|C}(t)$ is dominated by the variation of the predicted process N_a, whereas the variation due to the best predictor is negligible, that is

$$\begin{aligned}\mathrm{var}\{d\varepsilon_{a|C}(t)\} &= \mathrm{var}\{\mathrm{d}N_a(t)\} + \text{terms of order } \mathrm{d}t^2 \\ &= p_a\mathrm{d}t + \text{terms of order } \mathrm{d}t^2\end{aligned}$$

This leads to the following definition of the scaled partial covariance density (SPCD)

$$s_{ab|C}(u) = \frac{q_{ab|C}(u)}{\sqrt{p_a p_b}}$$

Like the conditional intensity, the scaled partial covariance density gives information not only on the strength of a connection between two neurons but also on the type and the direction of the connection. For an

excitatory connection from neuron b to neuron a the time delay u_0 due to the propagation of the action potential along the axon and the synaptic delay results in a peak of $s_{ab|C}(u)$ at $u = u_0$. Similarly, for an inhibitory connection we obtain a trough at $u = u_0$.

The partial spectra and partial spectral coherences can be estimated by replacing the spectral densities $f_{ij}(\lambda)$ in Eq. 2 by their estimates $\hat{f}_{ij}^{(T)}(\lambda)$. For a multivariate point process N with components N_a, $a = 1, \ldots, d$, all partial spectral coherences $|R_{ab|V\setminus\{a,b\}}(\lambda)|^2$ with $V = \{1, \ldots, d\}$ can be computed efficiently by inversion of the spectral matrix (Dahlhaus 2000). Let $g(\lambda) = (g_{ab}(\lambda))_{a,b=1,\ldots,d}$ denote the inverse spectral matrix. Then we have

$$f_{aa|V\setminus\{a\}}(\lambda) = \frac{1}{g_{aa}(\lambda)}$$

$$R_{ab|V\setminus\{ab\}}(\lambda) = -\frac{g_{ab}(\lambda)}{\sqrt{g_{aa}(\lambda)g_{bb}(\lambda)}}$$

$$f_{aa|V\setminus\{ab\}}(\lambda) = \frac{f_{aa|V\setminus\{a\}}(\lambda)}{1 - |R_{ab|V\setminus\{ab\}}(\lambda)|^2}$$

$$f_{ab|V\setminus\{ab\}}(\lambda) = \frac{R_{ab|V\setminus\{ab\}}(\lambda)}{1 - |R_{ab|V\setminus\{ab\}}(\lambda)|^2} \times \sqrt{f_{aa|V\setminus\{a\}}(\lambda) f_{bb|V\setminus\{b\}}(\lambda)}$$

The first two equations have been proved by Dahlhaus (2000), while the other two equations follow from these and the inverse variance lemma (e.g. Whittaker 1990, Prop. 5.7.3). Replacing the spectral matrix by its estimate we obtain estimates for all partial second-order statistics in the frequency domain. Further, we can estimate the partial covariance density $q_{ab|C}(u)$ for $a \neq b$ by the Fourier transform of the partial spectral density estimate:

$$\hat{q}_{ab|C}^{(T)}(u) = \int_{-\pi/b_T}^{\pi/b_T} \hat{f}_{ab|C}^{(T)}(\lambda) \exp(-\mathrm{i}u\lambda)\, \mathrm{d}\lambda \tag{3}$$

where b_T converges to zero as $T \to \infty$. The properties of the estimate can be further improved by the introduction of a convergence factor $\gamma_T(\lambda)$, which is monotonically decreasing in λ and increasing in T. Finally, the scaled partial covariance densities can be estimated by substituting the empirical means $\hat{p}_a^{(T)} = N_a(T)/T$ for the mean intensities p_a.

2.3 Partial correlation graphs

Partial second-order statistics can be used for the definition of undirected graphs that visualize the correlation structure of a multivariate point process. Such partial correlation graphs have been used by Dahlhaus et al. (1997) for the identification of synaptic connections from neural spike train data. A detailed discussion of partial correlation graphs and their properties in the context of multivariate time series can be found in Dahlhaus (2000). The same results also hold for point processes.

Suppose that we observe a multivariate point process $N = (N_1, \ldots, N_d)'$. We identify the components N_a with the vertices of a graph, i.e., we have the set of vertices $V = \{1, \ldots, d\}$. An edge between vertices a and b is defined to be missing if the corresponding processes N_a and N_b are uncorrelated at all lags after the linear effects of all other components have been subtracted. With the definitions of the last section this is the case if and only if the partial residual processes $\varepsilon_{a|V\setminus\{a,b\}}$ and $\varepsilon_{b|V\setminus\{a,b\}}$ are uncorrelated at all lags and consequently the scaled partial covariance density $s_{ab|V\setminus\{a,b\}}(u)$ is zero for all u.

In practice, the partial correlation graph must be estimated from the empirical scaled partial covariance densities

$$\hat{s}_{ab|V\setminus\{a,b\}}^{(T)}(u) = \frac{\hat{q}_{ab|V\setminus\{a,b\}}^{(T)}(u)}{\sqrt{\hat{p}_a^{(T)}\hat{p}_b^{(T)}}}$$

which in the case of a missing edge are only approximately zero. Therefore, statistical tests must be employed to decide whether an edge is missing. This can be done by constructing a threshold for the empirical scaled partial covariance density. If this threshold is exceeded for some lag u, we decide that there is an edge between vertices a and b.

An approximate threshold can be obtained from the asymptotic distribution of $\hat{s}_{ab|V\setminus\{a,b\}}^{(T)}(u)$. In the appendix, we show that under the hypothesis of $s_{ab|V\setminus\{a,b\}}(u) = 0$ and under the further assumption that $b_T \to 0$ and $Tb_T \to \infty$ as $T \to \infty$ the empirical scaled partial covariance density is asymptotically normal with mean zero and variance

$$\lim_{T\to\infty} Tb_T \mathrm{var}\{\hat{s}_{ab|V\setminus\{a,b\}}^{(T)}(u)\} = H_4/H_2^2$$

We note that the asymptotic variance does not depend on the process N, which is a consequence of the chosen scaling. As a measure of the detectability of an interaction between two processes we use the detectability index D (Aertsen and Gerstein 1985), which is defined by $D = d/\sigma$, where d is the absolute amplitude of the maximum peak or trough of $\hat{s}_{ab|V\setminus\{a,b\}}^{(T)}(u)$ and σ^2 is the above asymptotic variance.

For a neural network the partial correlation graph derived from the spike trains does not directly reflect the physiological connectivity structure of the network. The connectivity of the network can be described by a directed graph in which a directed edge from a to b is present if and only if there is a neural pathway from neuron a to neuron b that does not involve any of the remaining neurons in V. In this case, we say that a is a parent of b and b is a child of a. The edges in the partial correlation that indicate linear relationships between the spike trains now do not necessarily coincide with the edges in the directed graph since for converging connections the input processes become correlated after partialization. Thus, in the directed graph all parents of a joint child must be connected by an edge in order to

get the partial correlation graph. This so-called moralization of the directed graph is well known in the theory of graphical models (Whittaker 1990).

Dahlhaus et al. (1997) have shown that partial correlation graphs nevertheless can be used for the identification of the synaptic connectivities by application of a recursive procedure. This procedure is based on the observation that for a directed graph without cycles all terminal vertices, i.e., vertices without children, and their adjacent edges can be correctly identified from the scaled partial covariance density. After these vertices have been removed from the vertex set, the partial correlation graph for the remaining vertices is estimated and the terminal vertices in the new graph are determined. By recursion of this scheme all directed edges can eventually be identified.

2.4 Simulation

A network of simulated neurons has been used to investigate the properties of the proposed partial correlation analysis. The spike trains of the model neurons are described by a stochastic point process N generated from a nonlinear integrate-and-fire model with refractory period. An extensive discussion of the model, in terms of stochastic equations, is given in Johannesma and van den Boogaard (1985).

Let $\tau_a(t)$ denote the last time neuron a has fired before time t. Then the intracellular potential of neuron a is given by

$$u_a(t) = \sum_{b=1}^{d} \int_{\tau_a(t)}^{t} w_{ab}(t-u)\,\mathrm{d}N_b(u) \tag{4}$$

The weight functions $w_{ab}(u)$ determine the size and shape of the postsynaptic potential for the connection from neuron b to neuron a. In the simulations, an exponential shape has been chosen for the weight functions

$$w_{ab}(u) = w_{ab} \exp\big(-(u-u_{ab})/\sigma_{ab}\big)$$

for $u > u_{ab}$ and zero elsewhere. The amplitude factor w_{ab} measures the strength of the connection and also indicates whether the link is excitatory or inhibitory. Furthermore, u_{ab} is the time delay of the connection and σ_{ab} determines the duration of the postsynaptic potential. In the case $a = b$, the integral in Eq. 4 becomes $w_{aa}\big(t-\tau_a(t)\big)$ and models the refractoriness of the neuron.

The probability that an output spike of type a is generated can be written as

$$\mathrm{Prob}\{\mathrm{d}N_a(t) = 1 | u_a(t) = u\} = g_a(u)\,\mathrm{d}t$$

where the pulse generator function $g_a(u)$ is of exponential shape:

$$g_a(u) = \mu_a \exp(u)$$

The constant μ_a determines the spontaneous firing rate.

2.5 Local neuronal connectivity in spinal cord

The proposed method has been used to analyze neuronal spike trains from ten simultaneously recorded neurons. Methods have been described in detail elsewhere (Sandkühler and Eblen-Zajjur 1994). In brief, multiple single neuron recordings were made with tungsten microelectrodes (impedance 4–5 $M\Omega$) in deep layers of lumbar spinal cord of adult, pentobarbital anaesthetized Sprague-Dawley rats. Spinal cord was transected rostral to the recording sites to remove any descending inhibition and facilitation from supraspinal sites. Recordings were digitized at 32 kHz by an A/D converter card (Data-Translation DT2821). Discrimination of action potentials from individual neurons was made with the principal component method based on the shape of the waveform using the Discovery software package version 3.1 (BrainWave Sytems). Background activity in the absence of intentional stimulation was recorded for 10–30 min to collect 2000–5000 action potential discharges of each neuron under study.

3 Results

3.1 Comparison of SPCD and SCD

In order to illustrate the effect of partialization on the association of neural spike trains, we have simulated various networks of three neurons using the integrate-and-fire-model described in Sect. 2.4. The scaled partial covariance densities $s_{21|3}(u)$ and the scaled covariance densities $s_{21}(u)$ estimated from the simulated data are given in Fig. 1.

In the first two networks (a) and (b), neurons 1 and 2 are directly connected. In this case, partialization has no effect on the linear relationship of N_1 and N_2 and the diagrams for the SPCD and the SCD are virtually the same. The results are different if the two neurons are connected indirectly via a third neuron as in networks (c) and (d). For these networks the peak (trough) in the SCD indicating an excitatory (inhibitory) connection vanishes after the linear effects of the intermediate process have been removed. The same effect can be observed for networks (e) and (f) with diverging connectivities after partialization on the common input. Altogether the SPCD correctly distinguishes direct connections from indirect connections and common inputs.

The next two examples (g) and (h) show that for networks with converging connections the behavior of the SCD and the SPCD is contrary to the case of diverging connections. In this case, the SCD between the input processes does not show any significant deviation from zero, whereas after partialization on the output process the input processes become correlated. This so-called marrying-parents effect (Dahlhaus et al. 1997) leads to a central trough in the SPCD if the two inputs are of the same type, while for inputs of opposite types the SPCD has a central peak.

In practice, the activity of only a small part of the neural network can be measured simultaneously. In

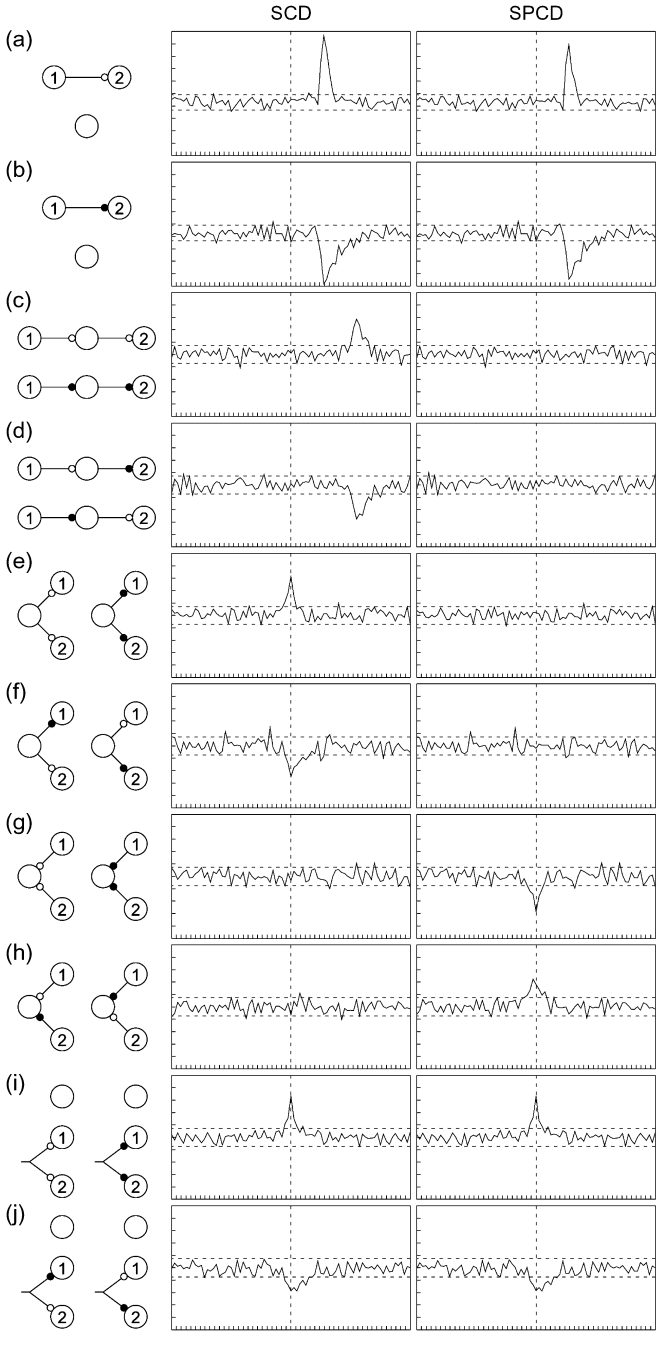

Fig. 1. SCD (*left*) and SPCD (*right*) for three different neuron networks. The *horizontal dashed lines* signify pointwise 95% thresholds for the hypothesis that the scaled (partial) covariance density is zero

general, we cannot infer by partial correlation analysis to what extent an association between two spike trains is due to a direct connection between the corresponding neurons or only the result of an incomplete monitoring of the network since it is not possible to remove the linear effects of neurons whose activity has not been recorded. Therefore, the partial correlation analysis only reveals the connectivity relative to the set of monitored neurons. However, if the SPCD has a central peak or trough, the SCD can be used to distinguish between the two possible causes: if the peak or trough vanishes in the SCD, it has been due to a marrying-parents effect. On the other hand, if the peak is also visible in the SCD, this signifies a common input from outside the measured network, as depicted in (i) and (j).

3.2 Detectability of SPCD

The next two sets of simulations have been performed to evaluate the limitations of the partial correlation analysis for the discrimination of the connectivity patterns discussed in the previous section. In the first set of simulations, we studied the sensitivity of the SPCD and the SCD on the strength of connectivity and the neural activity. The simulation with recording time $T = 60$ s is based on 100 replications for each configuration. The results for three neuron networks with direct, indirect, and converging connectivities are summarized in Fig. 2.

For direct connections (first two rows) the detectability curves have approximately the same shape for the SPCD and the SCD, although in the case of inhibition the detectability is slightly deteriorated by partialization. If the connectivity strength is increased, both types of connectivities become better detectable but the maximum of detectability shifts to lower intensities. This shift can be explained by superposition of postsynaptic potentials (see, e.g., Melssen and Epping 1987). Comparing the detectability of excitatory and inhibitory connectivities, the former were always better detectable than the latter ones. This observation is in accordance with previous findings for the crosscorrelation histogram by Aertsen and Gerstein (1985) and Melssen and Epping (1987).

The third row shows that in the case of excitation, the SPCD can discriminate direct and indirect connectivities over a large range of intensities. While for weak connectivities ($|w_{ab}| = 1$) the association due to indirect connectivities can be completely eliminated by partialization, significant peaks appear in the SPCD for intensities $\mu_a \geq 64$ Hz and $\mu_a \geq 128$ Hz, respectively, if the strength of connectivity is increased. For these parameters the impulse transmission becomes more deterministic, which prevents the discrimination of direct and indirect connections. In fact, in a purely deterministic system, the firing pattern of an indirect connection from a to c via b would be the same as that of a common input of a on b and c, thus making an indirect and a direct connection between a and c indistinguishable. Still, partialization causes a substantial reduction of the detectability and thus reveals that the timing relation between the two spike trains is dominated by an indirect connectivity. In the case of inhibition, direct and indirect connections are correctly discriminated by the SPCD irrespective of the firing rate and the connectivity strength. However, it should be noted that Melssen and Epping (1987) observed situations in which inhibitory connectivities have a much improved detectability, which may lead to a similar behavior as in the case of excitation.

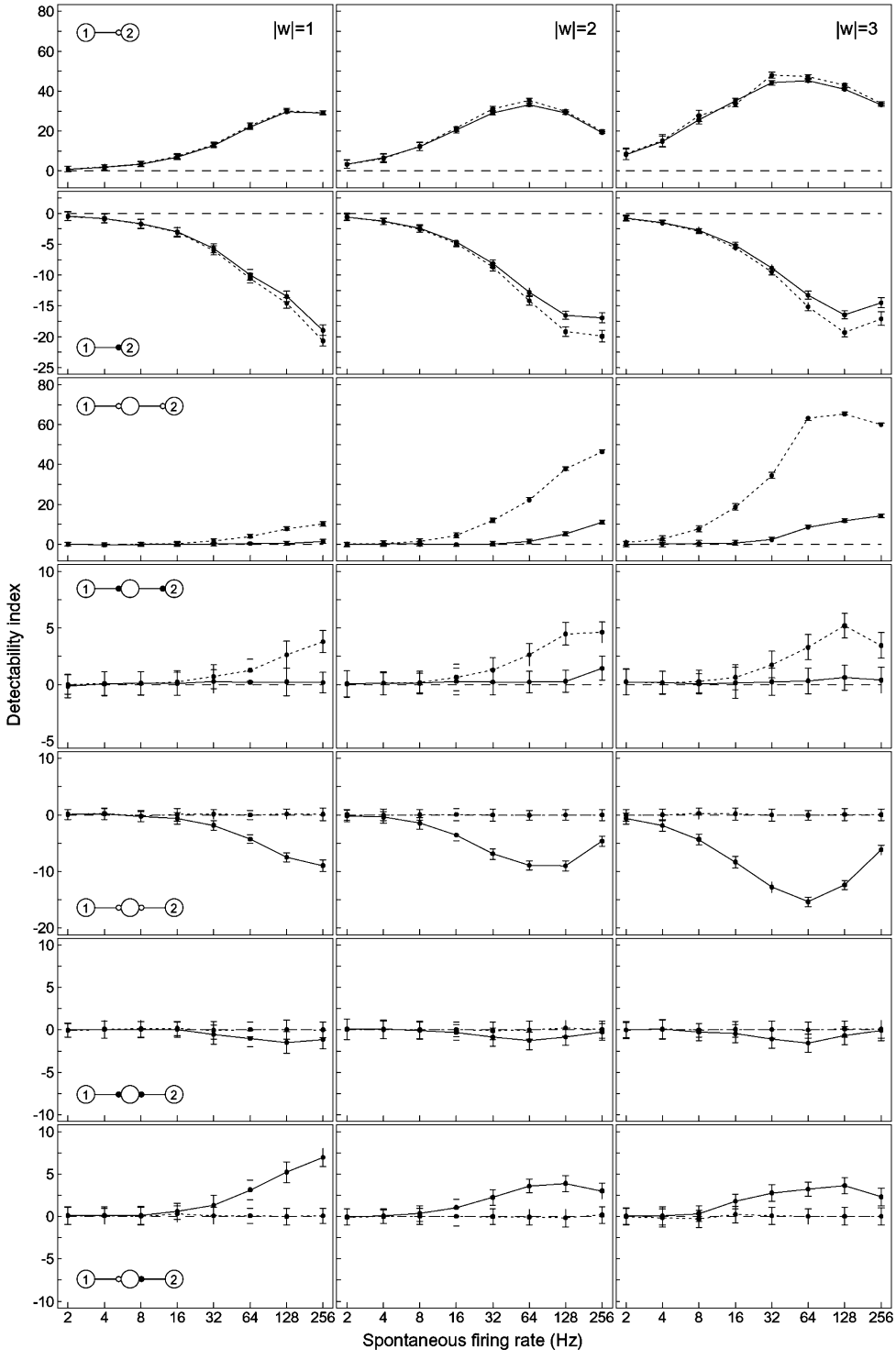

Fig. 2. Detectability of synaptic connections: detectability index (mean ± SD) of SPCD (*solid lines*) and SCD (*dashed lines*) at maximal peak or trough for direct connections, indirect connections, and converging connections. *Horizontal axis*: spontaneous activity of the neurons

In the case of converging connectivities (last three rows), the shape of the detectability curves of the SPCD is similar to the shape for direct connectivities, but the detectability index is significantly smaller at all intensities and for all connectivity strengths. In particular, if both converging connections are inhibitory, the resulting trough in the SPCD is hardly discernible for any intensity. The different detectability for direct and converging connectivities is important as it allows the complete identification of the converging structure in the network whenever a marrying-parents effect leads to a significant peak or trough in the SPCD. Since the SCD does not show any significant deviation from zero irrespective of intensity or connectivity strength, the converging connectivity can finally be distinguished from a common input from outside the monitored network by an appropriate reduction of the network.

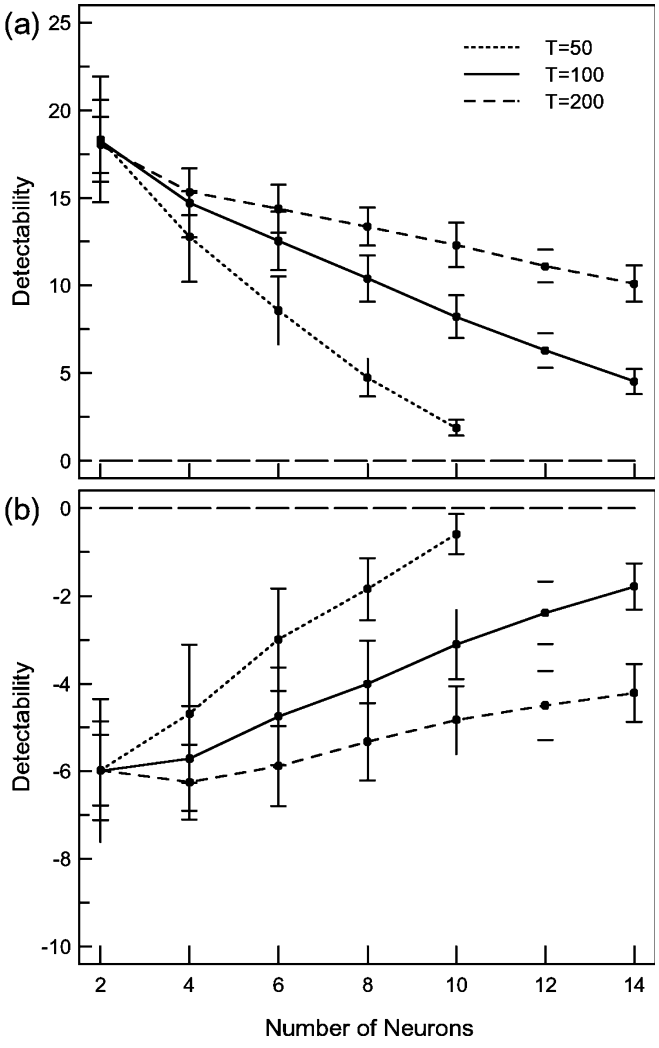

Fig. 3. Detectability of synaptic connections: detectability index (mean ± SD) of SPCD for different recording times [$T = 50$ s (*dotted*), $T = 100$ s (*solid*), $T = 200$ s (*dashed*)] estimated from different number of neurons for excitatory connection **(a)** and inhibitory connection **(b)**

In the second set of simulations we investigated the effect of the number of recorded neurons on the detectability of direct connectivities by partialized statistics. For this we considered networks that consisted of two directly connected neurons and a varying number of totally disconnected neurons. Figure 3 depicts the detectability of excitatory and inhibitory connectivities as a function of the number of neurons included in the study for three different recording times ($T = 50$ s,100 s, and 200 s). For both types of connections the detectability curve exhibits a strong dependence on the number of neurons and the recording time. The detectability is diminished by an increase of the size of the networks up to some breakpoint at which connectivities become totally undetectable. For sampling length $T = 50$ s this breakpoint occurs at a network size of 11 and 10 neurons for excitatory and inhibitory connectivities, respectively. If the recording time is increased, the detectability improves and the breakpoint shifts to higher numbers of neurons. This deterioration of the

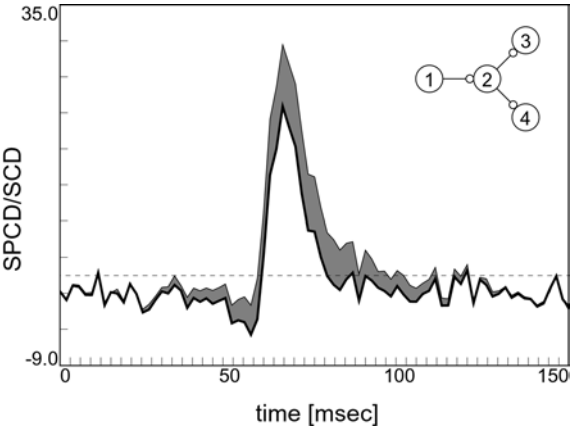

Fig. 4. SPCD (*bold*) and SCD (*shaded*) for the direct connection between model neurons 1 and 2 in a four-neuron network for $T = 500$ s

detectability in large networks is caused by the finite length of the spike train recordings. This allows for the features in the realization to be reproduced arbitrarily well by a linear combination of a sufficiently large number of, e.g., Poisson processes. Therefore, if the number of neurons increases, partialization eventually leads to the total elimination of any information on a direct connectivity between two neurons.

If the number of connectivities in the measured network increases, the detectability can be further diminished by partialization even for very long recordings of the spike trains. This effect is due to partialization on succeeding neurons and thus related to the marrying-parents effect described in the previous section. To illustrate the effect, we simulated a network of four connected neurons (Fig. 4) with sample period $T = 500$ s. The SCD and the SPCD for the direct connection from neuron 1 to neuron 2 are displayed in Fig. 4. The area between the curves signifies the decrease in detectability if the SPCD is used instead of the SCD. Despite the long recording, we observe a reduction in height of about 25% over the full width of the peak. This reduction can be explained as follows: the spike trains of neurons 3 and 4 improve the prediction of the firing times of neuron 2 since both neurons are excited by neuron 2. Therefore, partialization on neurons 3 and 4 decreases the probability for a discharge of neuron 2 if this is followed by a discharge in neuron 3 or 4. More precisely, the partial residual process $\varepsilon_{2|3,4}(t)$ has a smaller mean intensity than the spike train $N_2(t)$. The same holds if we consider instead the conditional mean intensity of $\varepsilon_{2|3,4}(t)$ given that neuron 1 has fired, which is equivalent to the SPCD. Just as for the marrying-parents effect, the reduction is approximately symmetric and therefore causes a small trough, which precedes the asymmetric peak on its steep side.

3.3 SPCD for multiple connections

We examined the ability of partialization analysis in the time domain to detect multiple direct connections

between two neurons. For this we analyzed data from a simulated network of six neurons with an excitatory feedback loop (Fig. 5a). Such circuits have been used as a model for the short time memory. The same data have been analyzed by Dahlhaus et al. (1997) with frequency domain methods in the case where only neurons 1, 2, 4, and 6 are monitored. In this reduced network, neurons 2 and 4 are joined by two direct connections of opposite directions.

Figure 5c and d presents the results of the frequency domain analysis. The partial spectral coherence $|R_{4,2|1,6}(\lambda)|^2$ (Fig. 5c) correctly detects that neurons 2 and 4 are directly connected. The slope of the corresponding partial phase spectrum (Fig. 5d) now indicates that impulses are transmitted in the direction of neuron 4, which corresponds to the main pathway in the network. Neither the partial coherence nor the partial phase provide any information about the presence of an excitatory feedback connection.

The corresponding partialized time domain statistic $s_{2,4|1,6}(u)$ is depicted in Fig. 5b. We observe two distinct peaks at lag $u = 36$ ms and at lag $u = -36$ ms, which correctly indicates that impulses between the two neurons are transmitted in both directions. Both connections are excitatory and have approximately the same time delay. Thus the SPCD leads to a complete identification of the connectivity structure. Comparing the height of the peaks we further find that the signal transmission in the direction of neuron 4 is slightly stronger. Therefore, the averaged time delay of the linear relationship between the two spike trains is positive, which explains the negative slope of the partial phase spectrum.

3.4 Temporal variation of neuronal interactions

The SCD and SPCD are average measurements for the effective connectivity over the entire length of the recorded data. Their validity therefore depends on the stationarity of the recorded spike trains. However, in many experimental situations, the network shows dynamic activity due to, for example, behavior or sensory stimulation. In such situations, the firing rates and correlations between neurons may vary dramatically even in sign (e.g., Aertsen and Gerstein 1985; Vaadia et al. 1991). Such modifications of neuronal interactions can be exposed by segmenting the data into shorter sections and computing the estimates from the data in each section. Plotting the results as a function of time we can assess the temporal variation of the neuronal interactions.

For illustration purposes we have simulated a network of three neurons in which the spontaneous firing rates μ_a and the amplitude factors w_{ab} varied randomly over time. For each component the firing rate and the amplitude factor were obtained from a Markov process with two states: high or low for the firing rate and positive or negative for the amplitude factor. The connectivity of the network is depicted in Fig. 6; the total simulation period was 500 s.

The partialization analysis based on the entire data (Fig. 6b) reveals three excitatory direct connections, while the second peak in the SCD between neurons 1 and 3 is correctly attributed to an indirect connection via neuron 2. Additionally, for neurons 2 and 3 both SCD and SPCD show a peak at the origin, which indicates the presence of a common input from an unmeasured source. To investigate the temporal variation of the dependence structure we have computed the time-varying SPCD and SCD from overlapping segments of length 20 s and shift 2.5 s (Fig. 6a). Here the changes along the vertical axis reflect the nonstationarity of the functional relationships between the processes. In particular, we find that the direct connection between neurons 1 and 3 is not purely excitatory but becomes inhibitory over the last 150 s of the simulations. From the plot we can identify time intervals over which the

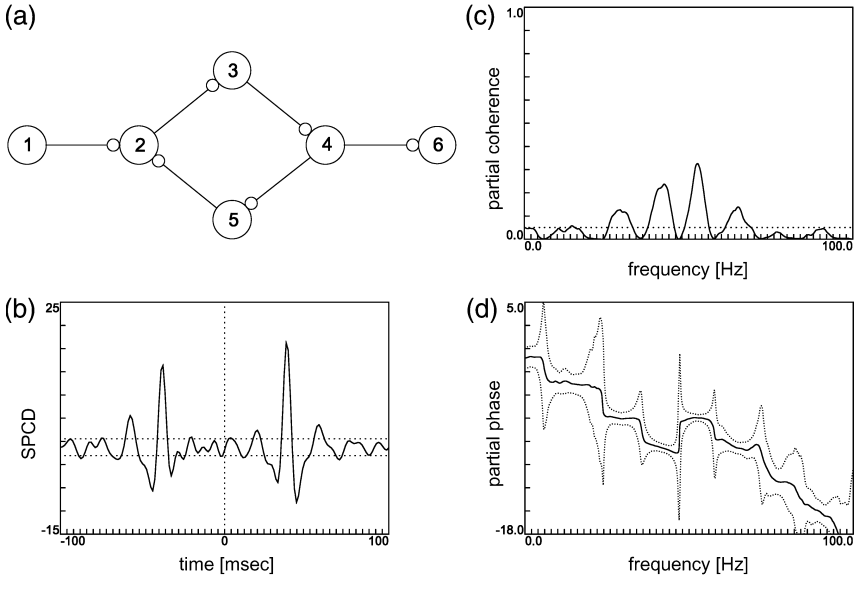

Fig. 5. Identification of multiple connections of opposite directions. **a** Simulated network with excitatory feedback. **b** Estimated SPCD $\hat{s}_{4,2|1,6}(u)$. **c** Estimated partial coherence $|\hat{R}_{4,2|1,6}(\lambda)|^2$. **d** Estimated partial phase $\hat{\phi}_{4,2|1,6}(\lambda)$ with 95% confidence interval

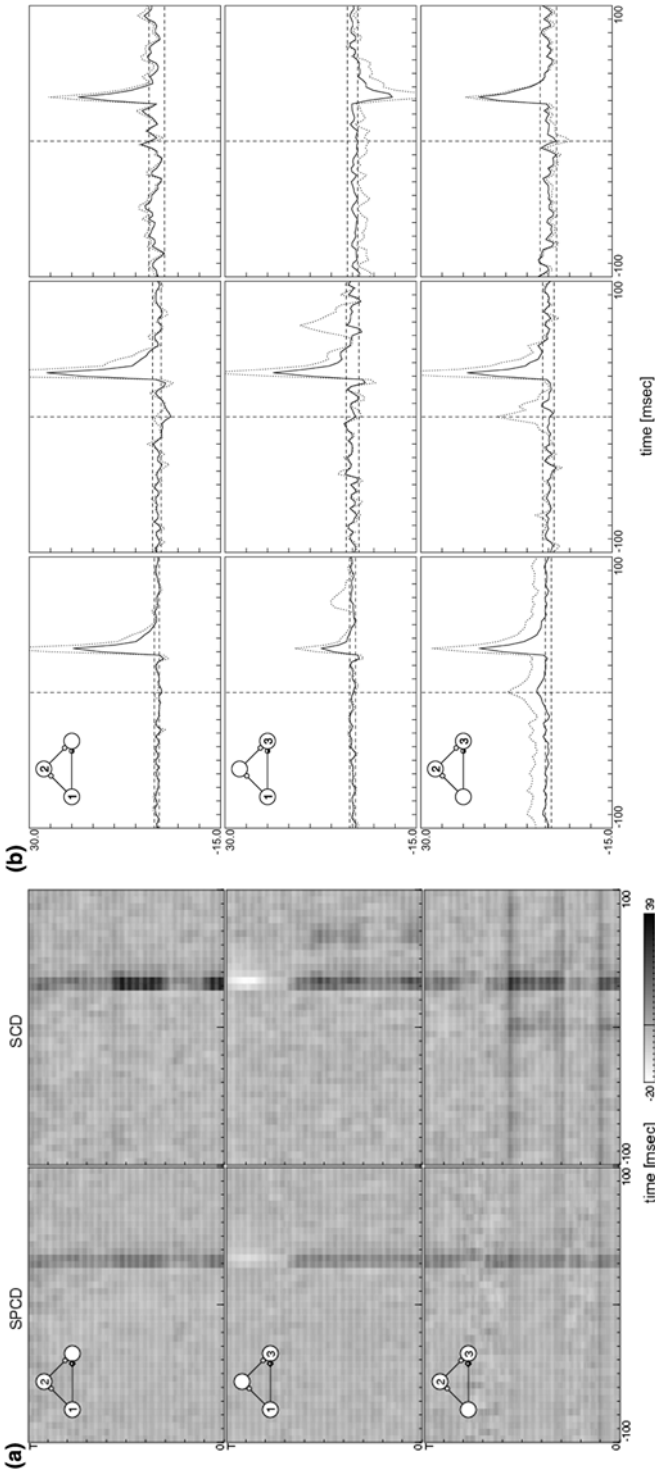

Fig. 6. **a** Estimated time-varying SPCD and SCD for simulated three-neuron network. **b** Estimated SPCD (*solid*) and SCD (*dotted*) for simulated three-neuron network for different sampling periods: 0–500 s (*left*), 150–250 s (*middle*), and 350–500 s (*right*)

processes seem to be approximately stationary. For two such intervals (150–250 s and 350–500 s) we have computed SPCD and SCD to analyze the effective connectivity of the network at these times. As can be seen in Fig. 6b, the analysis of these shorter segments leads to a correct identification of the network. In particular, we note that the results reject the presence of a common input for neurons 2 and 3 as the peak at the origin of the SPCD has vanished.

3.5 Partial correlation analysis of measured spike trains

Finally, we analyzed spike train data from the lumbar spinal dorsal horn of a pentobarbital-anaesthetized rat during noxious stimulation. The firing times of ten neurons were recorded simultaneously by a single electrode with an observation time of 100 s. The data have been measured and analyzed by Sandkühler and Eblen-Zajjur (1994), who studied discharge patterns of spinal dorsal horn neurons under various conditions.

Figure 7b displays the estimated SCD and SPCD for the ten neurons. The SCD shows for 32 (71%) pairs of neurons a peak at or near the origin. In 18 (40%) cases, these peaks are accompanied by smaller bilateral peaks. From the estimated autospectra (Fig. 7a) we find that these smaller peaks are associated with rhythmic discharges at 5 Hz in one or both neurons, which corresponds to the observed time lag of 200 ms to the main peak.

A much clearer picture of the connectivity structure is provided by the SPCD. The majority of the peaks present in the SCD have disappeared after partialization. Only for nine pairs of neurons do we observe a highly significant peak at $u = 12$ ms preceded by a smaller trough. These troughs may be due to either partialization on successive neurons as described in Sect. 3.2 or the periodic firing of the neurons, which in general leads for a direct connection to a similar combination of peak and trough. In the latter case, the trough appears also in the SCD as, for example, for neurons 8 and 10, but the difference in the depth of the trough in the SCD and in the SPCD may still be due to partialization. Furthermore, only two pairs exhibit small bilateral peaks besides the sharp main peak. These can be ascribed to the strong periodicity of discharges of neuron 1, which is included in both pairs. Additionally, we find a small central trough for the SPCD between neurons 1 and 3.

To identify the connectivities for this set of the neurons, we apply the recursive identification procedure by Dahlhaus et al. (1997). In the first step, we estimate the partial correlation graph (Fig. 8a) using the approximate threshold for the SPCD derived in Sect. 2.3. To determine the terminal vertices, i.e., vertices that have no adjacent edges pointing to other edges, in the underlying directed graph, we identify preliminary directions for the edges from the lags of the peaks and troughs. The nine peaks are interpreted as direct excitatory connections between the neurons according to the remarks above, whereas the direction of the edge associated with the central trough remains open. Figure 8b shows the determined terminal vertices and the identified final directions for the adjacent edges. In the next step, the terminal vertices are removed from the vertex set and the partial correlation graph is estimated from the SPCD for

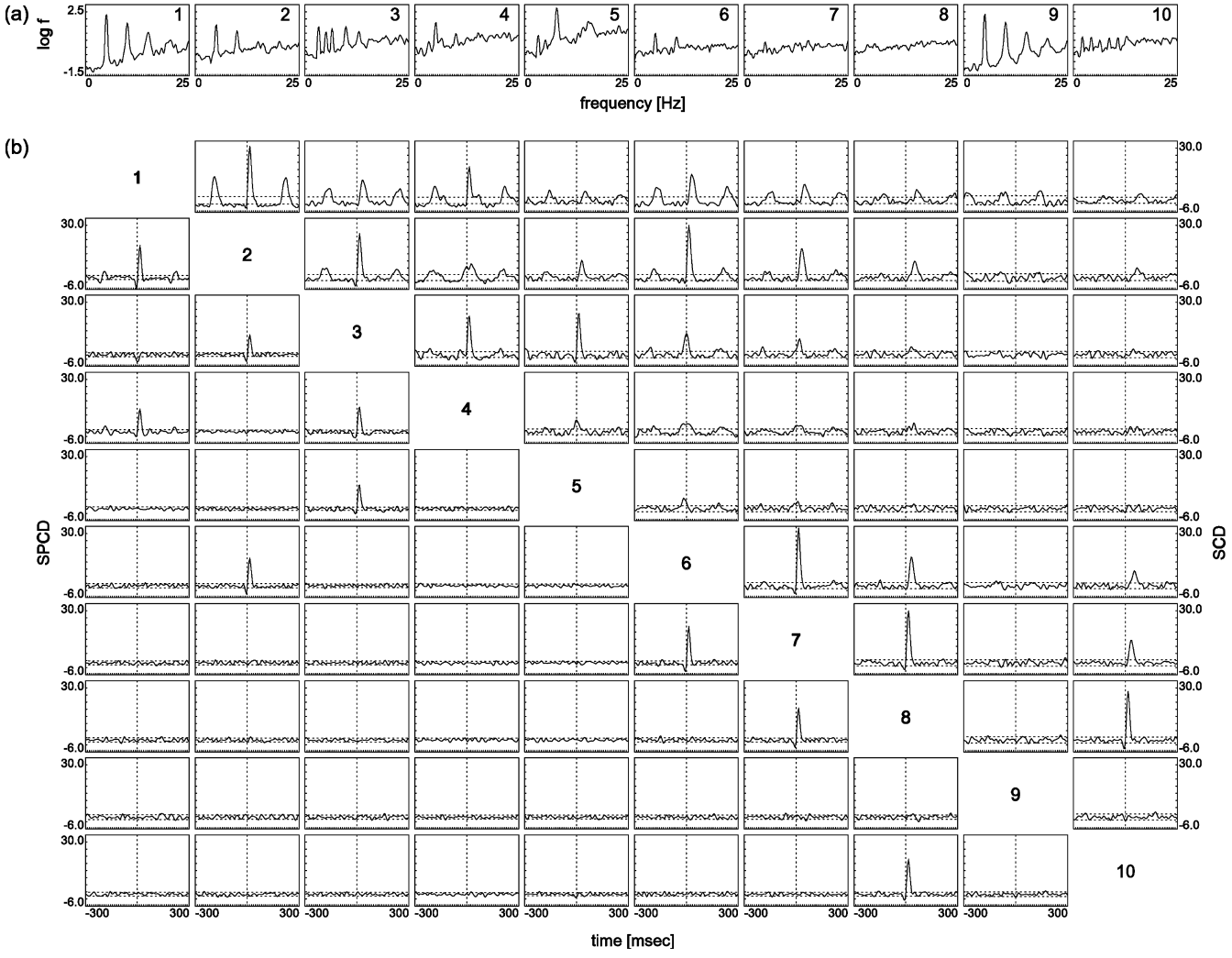

Fig. 7. a Logarithm of spectral densities for spinal dorsal horn neurons 1 to 10. **b** Scaled partial covariance densities (*below diagonal*) and scaled covariance densities (*above diagonal*) for spinal dorsal horn neurons 1 to 10. The *horizontal dotted lines* signify pointwise 95% thresholds for the hypothesis that the scaled (partial) covariance density is zero

the thus reduced set of neurons. In the SPCD between neurons 1 and 3 (Fig. 9), the trough has now disappeared. Therefore, the edge between 1 and 3 in the original partial correlation graph has been due to the converging of the connections from neurons 1 and 3 to neuron 4. Since for all other pairs the SPCD remains basically the same, we obtain the partial correlation graph in Fig. 8c. Repeating the recursive scheme three more times the final directions of all edges are determined and we obtain the connectivity graph in Fig. 8d as the final estimate of the connectivities between the neurons.

Comparing the connectivity graph with the SCD we find that neuron 9 is totally disconnected from the other neurons, although it is weakly correlated with neurons 1 and 2. The autospectra (Fig. 7a) reveal that all three neurons exhibit a strong periodicity at 5 Hz. Therefore, the time lags between successive discharges tend to be the same for these neurons, which then leads to a correlation that is not associated with a connectivity.

We note that this graph displays only the relative connectivity structure, and it cannot be excluded that some or all of the direct connections are only due to indirect connectivities or common inputs involving unmeasured neurons. Nevertheless, the results allow one to falsify certain hypotheses that are in conflict with the estimated graph. For example, the periodic behavior of many of the measured neurons might suggest one common input for those neurons. In that case, the corresponding subset of vertices in the connectivity graph must be complete, that is, any two vertices in the subset are joined by an edge. This is clearly not the case for the estimated connectivity graph in Fig. 8d.

Finally, we computed the time-varying SPCD and SCD to check for temporal variation in the effective connectivity of the network. Here we only give the results for neurons 1–5, plotted in Fig. 10, but the results for the complete network are similar. The shapes of SPCD and SCD appear stable over the entire observation period, and we therefore conclude that the

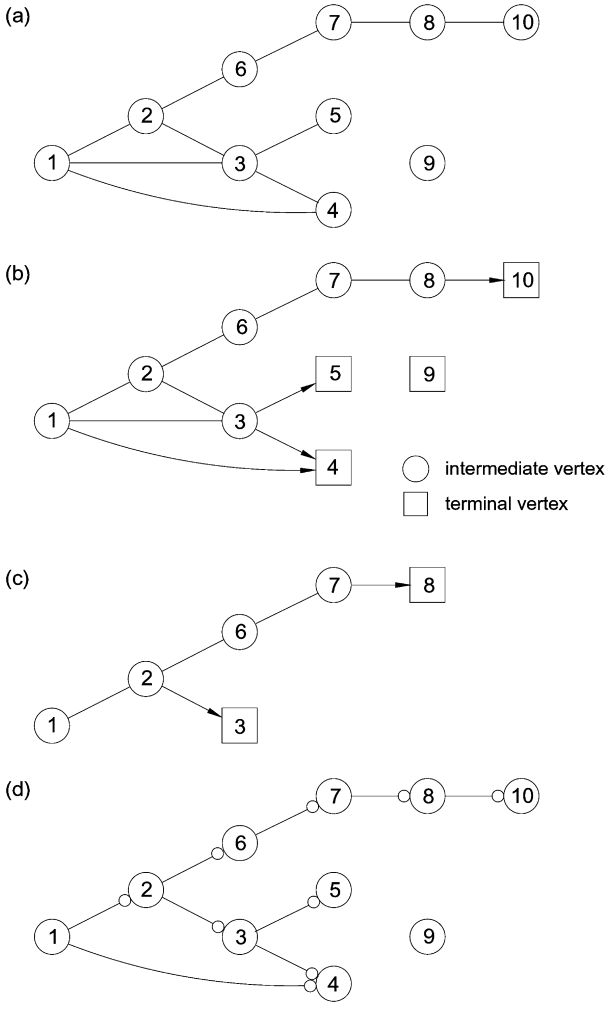

Fig. 8. **a** Estimated partial correlation graph for spinal dorsal horn neurons 1 to 10. **b** Identification of terminal vertices. **c** Reduced partial correlation graph for neurons 1, 2, 3, 6, 7, and 8 with identified terminal vertices. **d** Estimated connectivity graph for neurons 1 to 10

stationarity assumption for the above partialization analysis is fulfilled.

4 Discussion

We have seen that the scaled partial covariance density is a useful tool for the identification of functional connectivities in neural ensembles. Although the presented time domain techniques are mathematically equivalent to the frequency domain approach suggested by Brillinger et al. (1996), Rosenberg et al. (1989), and Dahlhaus et al. (1997), both methods emphasize distinct features of the data. We have shown that the SPCD can be used for the identification of the direction and the type of synaptic connections.

The results in this paper have shown that the detection of different neural configurations like direct, indirect, diverging, and converging connections depends on the signal-to-noise ratio of the measured spike trains. In particular, high ratios lead to a quasideterministic neural

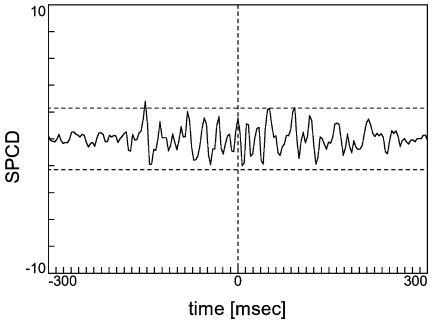

Fig. 9. Estimated SPCD $\hat{s}_{1,3|2,6,7,8}(u)$ for spinal dorsal horn neurons

coupling that prevents the discrimination of direct and indirect connectivities. Another limiting factor in the analysis of neural ensembles is the number of neurons included in the study. Partialization of an increasing number of neurons leads to deterioration of the detectability and eventually to the breakdown of the identification method. The effect can be compensated for by an increase of the sampling interval.

As we have emphasized before, the partialization statistics proposed in this paper measure only the effective connectivity between the observed neurons. Therefore, the connectivity graph obtained from a partialization analysis can replicate the true physiological connectivity only in a simplified way; direct connections, for example, may involve additional interneurons. Furthermore, only connections that were sufficiently active to be detectable at the time of observation are included in the connectivity graph.

These problems apply to steady-state experimental situations. Additional problems arise if firing rates and interactions between the neurons vary over time during behavior or sensory stimulation. For the evaluation of the temporal modifications of the functional relationships between the neurons we suggested applying the partialization method to short overlapping segments of the full spike trains and ploting the resulting statistics as functions over time. Naturally these statistics will have a lower precision, but they provide a rough picture of the temporal firing pattern and functionality of the network. In particular, the results may indicate time regions over which the process seems to be approximately stationary. The data from each of these regions can then be analyzed by the proposed partialization method.

Acknowledgements. The authors wish to thank an anonymous referee for his helpful comments on an earlier version of this paper.

Appendix

We give a short proof for the asymptotic distribution of the empirical SPCD. For the empirical SCD the asymptotic distribution has been derived by Rigas (1991). Let $C = V \backslash \{a, b\}$. We start by noting that under the assumptions of $s_{ab|C}(u) = 0$ the SPCD estimate $\hat{s}^{(T)}_{ab|C}(u)$ has the same limiting distribution as

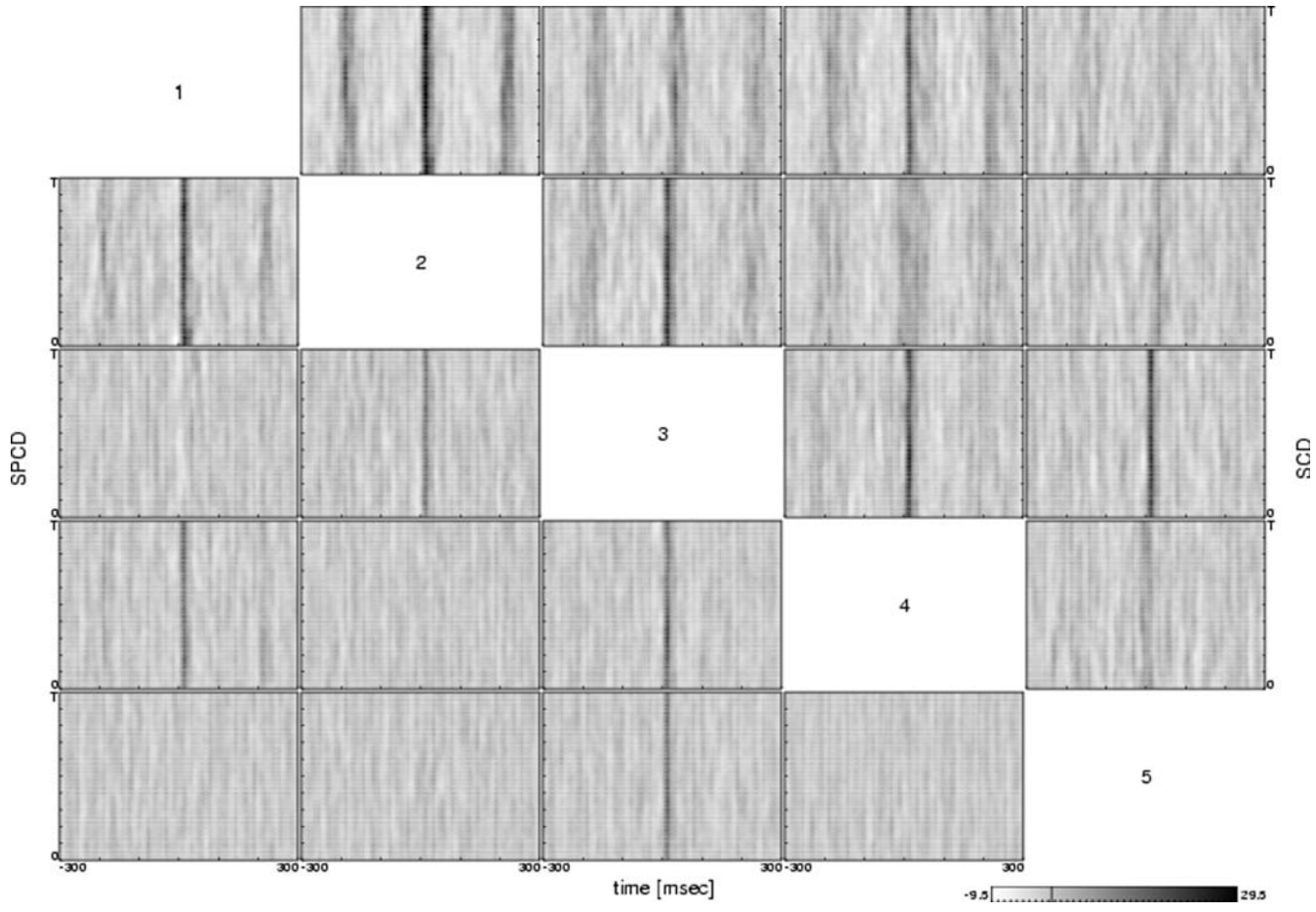

Fig. 10. Estimated time-varying SPCD and SCD for spinal dorsal horn neurons

$\hat{q}^{(T)}_{ab|C}(u)/\sqrt{p_a p_b}$

Since the partial cross-spectral density $f_{ab|C}$ is a nonlinear function of the entries of the spectral matrix $f = (f_{ij})$, the partial covariance density can be expressed as the integral of a nonlinear function of the spectral matrix. The asymptotic normality of estimates of such integrals of nonlinear functions of the spectral matrix has been proved by Taniguchi et al. (1996). Writing $D_{ij} = \partial f_{ab|C}/\partial f_{ij}$ we further obtain from the expression for the best predictor $\hat{N}_{a|C}(t)$ by elementary calculations that

$$\sum_{ij} D_{ij}(\lambda) f_{ij}(\lambda) = f_{ab|C}(\lambda),$$

$$\sum_{ijkl} D_{ij}(\lambda) D_{kl}(\lambda) f_{ik}(\lambda) f_{lj}(\lambda) = f_{ab|C}(\lambda) f_{ba|C}(\lambda),$$

$$\sum_{ijkl} D_{ij}(\lambda) D_{kl}(\lambda) f_{il}(\lambda) f_{kj}(\lambda) = f_{aa|C}(\lambda) f_{bb|C}(\lambda),$$

$$\sum_{ijkl} D_{ij}(\lambda) D_{kl}(\lambda) f_{ijkl}(\lambda, -\lambda, \mu) = f_{abab|C}(\lambda, -\lambda, \mu)$$

where f_{ijkl} and $f_{abab|C}$ are the fourth-order cumulant spectra of the multivariate process N and the bivariate partial residual process $\varepsilon_{ab|C}$, respectively. From the results in the cited paper it now follows that the partial covariance density estimate given by Eq. 3 is asymptotically normal with variance

$$Tb_T \mathrm{var}\left(\hat{q}^{(T)}_{ab|C}(u)\right)$$

$$= \frac{2\pi H_4 b_T}{H_2^2} \int_{-\pi/b_t}^{\pi/b_T} \int f_{abab|C}(\lambda, -\lambda, \mu) e^{\mathrm{i}u(\lambda-\mu)}\, \mathrm{d}\lambda\, \mathrm{d}\mu$$

$$+ \frac{2\pi H_4 b_T}{H_2^2} \int_{-\pi/b_t}^{\pi/b_T} f_{aa|C}(\lambda) f_{bb|C}(\lambda)\, \mathrm{d}\lambda \qquad (5)$$

Since $f_{abab|C}$ is absolutely integrable, the first term converges to zero as $b_T \to 0$. Further we have

$$f_{aa|C}(\lambda) = \frac{p_a}{2\pi} + \int_{-\infty}^{\infty} q_{aa}(u) \exp(-\mathrm{i}\lambda u)\, \mathrm{d}u$$

where the second term is absolutely integrable. Consequently, the second term in Eq. 5 converges to $(H_4/H_2^2)p_a p_b$, from which the stated asymptotic variance follows.

References

Aertsen AMHJ, Gerstein GL (1985) Evaluation of neuronal connectivity: sensitivity of crosscorrelation. Brain Res 340: 341–354

Aertsen AMHJ, Gerstein GL (1991) Dynamic aspects of neuronal cooperativity: fast stimulus-locked modulations of effective connectivity. In: Krüger J (ed) Neuronal cooperativity. Springer, Berlin Heidelberg New York

Alloway KD, Johnson MJ, Wallace MB (1993) Thalamocortical interactions in the somatosensory system: interpretation of latency and cross-correlation analyses. J Neurophysiol 70: 892–908

van den Boogaard HFP (1988) System identification based on point processes and correlation densities. II. The refractory neuron model. Math Biosci 91: 35–65

Brillinger DR (1981) Time series: data analysis and theory. McGraw Hill, New York

Brillinger DR (1996) Remarks concerning graphical models for time series and point processes. Revista de Econometria 16: 1–23

Brillinger DR, Bryant HL, Segundo JP (1976) Identification of synaptic interactions. Biol Cybern 22: 213–229

Cox DR, Isham V (1990) Point processes. Chapman & Hall, London

Dahlhaus R (2000) Graphical interaction models for multivariate time series. Metrika 51: 157–172

Dahlhaus R, Eichler M, Sandkühler J (1997) Identification of synaptic connections in neural ensembles by graphical models. J Neurosci Meth 77: 93–107

Daley DJ, Vere-Jones D (1988) An introduction to the theory of point processes. Springer, Berlin Heidelberg New York

Edwards D (1995) Introduction to graphical modelling. Springer, Berlin Heidelberg New York

Fetcho JR, O'Malley DM (1995) Visualization of active neural circuitry in the spinal cord of intact zebrafish. J Neurophysiol 73: 399–406

Gerstein GL, Aertsen AMHJ (1985) Representation of cooperative firing activity among simultaneously recorded neurons. J Neurophysiol 54: 1513–1528

Gerstein GL, Perkel DH, Dayhoff JE (1985) Cooperative firing activity in simultaneously recorded populations of neurons: detection and measurement. J Neurosci 5: 881–889

Gray CM, Maldonado PE, Wilson M, McNaughton B (1995) Tetrodes markedly improve the reliability and yield of multiple single-unit isolation from multi-unit recordings in cat striate cortex. J Neurosci Meth 63: 43–54

Grinvald A, Frostig RD, Lieke E, Hildesheim R (1988) Optical imaging of neuronal activity. Physiol Rev 68: 1285–1366

Hawkes AG (1971a) Spectra of some self-exciting and mutually-exciting point process. Biometrika 58: 83–90

Hawkes AG (1971b) Point spectra of some mutually exciting point processes. J R Statist Soc Ser B 33: 438–443

Johannesma PIM, van den Boogaard HFP (1985) Stochastic formulation of neural interaction. Acta Appl Math 4: 201–224

Kalitzin S, van Dijk BW, Spekreijse H, van Leeuwen WA (1997) Coherency and connectivity in oscillating neural networks: linear partialization analysis. Biol Cybern 76: 73–82

Krüger A (1983) Simultaneous individual recordings from many cerebral neurons: techniques and results. Rev Physiol Biochem Pharmacol 98: 176–233

Maeda E, Robinson HPC, Kawana A (1995) The mechanisms of generation and propagation of synchronized bursting in developing networks of cortical neurons. J Neurosci 15: 6834–6845

Melssen WJ, Epping WJM (1987) Detection and estimation of neural connectivity based on crosscorrelation analysis. Biol Cybern 57: 403–414

Perkel DH, Gerstein GL, Moore GP (1967) Neuronal spike trains and stochastic point processes. II. Simultaneous spike trains. Biophys J 7: 391–418

Rigas AG (1991) Spectra-based estimates of certain time-domain parameters of a bivariate stationary point process. Math Biosci 104: 185–201

Rigas AG (1992) Spectral analysis of stationary point processes using the fast Fourier transform algorithm. J Time Ser Anal 13: 441–450

Rosenberg JR, Amjad AM, Breeze P, Brillinger DR, Halliday DM (1989) The Fourier approach to the identification of functional coupling between neuronal spike trains. Prog Biophys Mol Biol 53: 1–31

Sandkühler J, Eblen-Zajjur AA (1994) Identification and characterization of rhythmic nociceptive and non-nociceptive spinal dorsal horn neurons in the rat. Neuroscience 61: 991–1006

Taniguchi M, Puri ML, Kondo M (1996) Nonparametric approach for non-gaussian vector stationary processes. J Multi Anal 56: 259–283

Vaadia E, Ahissar E, Bergman H, Lavner Y (1991) Correlated activity of neurons: a neural code for higher brain functions? In: Krüger J (ed) Neuronal cooperativity. Springer, Berlin Heidelberg New York

Whittaker J (1990) Graphical models in applied multivariate statistics. Wiley, Chichester